Published in final edited form as:
Radiother Oncol. 2013 October ; 109(1): 112–116. doi:10.1016/j.radonc.2013.07.015.

Motion-Specific Internal Target Volumes for FDG-Avid Mediastinaland HilarLymph Nodes

James M. Lamb[*,†,1], **Clifford G. Robinson**[*,2], **Jeffrey D. Bradley**[2], and **Daniel A. Low**[1]

[1]Department of Radiation Oncology, David Geffen School of Medicine, UCLA, Los Angeles, CA, USA

[2]Department of Radiation Oncology, Siteman Cancer Center, Washington University in St. Louis, St. Louis, MO, USA

Abstract

Background and Purpose—To quantify the benefit of motion-specific internal target volumes for FDG-avid mediastinal and hilar lymph nodes generated using 4D-PET, vs. conventional internal target volumes generated using non-respiratory gated PET and 4D-CT scans.

Materials and Methods—Five patients with FDG-avid tumors metastatic to 11 hilar or mediastinal lymph nodes were imaged with respiratory-correlated FDG-PET (4D-PET) and 4D-CT. FDG-avid nodes were contoured by a radiation oncologist in two ways. Standard-of-care volumes were contoured using conventional un-gated PET, 4D-CT, and breath-hold CT. A second, motion-specific, set of volumes was contoured using 4D-PET. Contours based on 4D-PET corresponded directly to an internal target volume (ITV_{4D}), whereas contours based on un-gated PET were expanded by a series of exploratory isotropic margins (from 5-13 mm) based on literature recommendations on lymph node motion to form internal target volumes (ITV_{3D}).

Results—A 13 mm expansion of the un-gated PET nodal volume was needed to cover the ITV_{4D} for 10 of 11 nodes studied. The ITV_{3D} based on a 13 mm expansion included on average 45 cm^3 of tissue that was not included in the ITV_{4D}.

Conclusions—Motion-specific lymph-node internal target volumes generated from 4D-PET imaging could be used to improve accuracy and/or reduce normal-tissue irradiation compared to the standard-of-care un-gated PET based internal target volumes.

Keywords

4D PET/CT; treatment planning; motion management; lung cancer; internal target volume

Introduction

Locoregional failure occurs in upwards of 50% of patients undergoing definitive chemoradiotherapy for locally advanced lung cancer[1,2], and such failures are an

[†]Corresponding author.
[*]These authors contributed equally to this manuscript.

Conflict of Interest Statement: No conflicts of interest.

independent driver of decreased overall survival after treatment[3]. Treatment of involved regional nodes only has become standard practice for most centers as a means to improve toxicity and allow for escalated doses of radiation[4,5]. Thus, accurate targeting of these nodes takes on even more importance in the absence of broad, elective treatment of the mediastinum. Lymph node motion is not generally measured in the treatment planning of advanced stage lung cancer, despite the fact that lymph nodes are known to move during respiration. Two recent studies[6,7] reported that over 10% of mediastinal and/or hilar lymph nodes moved at least 1 cm during respiration, as measured with 4D-CT, and furthermore that the motion amplitude at the same nodal station varied greatly between different patients and was not necessarily in phase with the motion of the primary tumor. Use of at least 5 mm margins to account for mediastinal lymph node motion has been recommended as standard clinical practice[8]. Sher et al[9] recommended that in the absence of node-specific motion information, margins of at least 8 mm, 13 mm, and 13 mm should be used to cover the internal target volume (ITV) of paratracheal, subcarinal, and hilar nodes, respectively. However, indiscriminate use of such population based margins could result in irradiation of excess normal tissue in many cases.

A 4D-CT scan can be used to compute a motion-specific nodal ITV, however there are certain drawbacks that make 4D-CT based node contouring unreliable and inefficient. Without contrast, lymph nodes can be difficult to identify, but contrast injection for 4D-CT is unreliable, because the long scan time of 4D-CT makes the timing of contrast injection difficult. Furthermore, 4D-CT is subject to well-known image artifacts[10]. Contouring of lymph nodes is more sensitive to the presence of artifacts, compared to primary tumors, because the lymph nodes are smaller. Finally, even when nodes are visible in 4D-CT images, it is time intensive to contour the nodes in several 4D-CT phase images. The time-saving procedure of contouring the primary tumor using the 4D-CT maximum intensity projection (MIP)[11] image in conjunction with end-exhale and end-inhale images is of limited utility for lymph nodes[12]. The 4D-CT MIP works well for primary tumors when they are surrounded by low-density lung parenchyma because the tumor always originates the highest intensity pixel value throughout all phases of the 4D-CT. It is less useful for lymph nodes because even if they are visible, the contrast between lymph nodes and the rest of the mediastinum is much less than the case of the isolated primary tumor. A similar problem occurs for primary tumors located near the chest wall or the diaphragm[11].

Positron emission tomography (PET) with 18F-fluorodeoxyglucose (FDG) has well-established utility in lung cancer radiotherapy planning[13]. The benefit of respiratory gating of PET for target volume delineation has been established in phantom studies[14], although un-gated PET is still more frequently used, in part due to logistical reasons related to the number of images produced. Aristophanous et al (2012)[15] recently reported on the potential clinical utility of 4D FDG-PET/CT for radiation treatment planning. They concluded that 4D-PET better defined the full physiologic extent of moving tumors compared to un-gated PET. Previously, we introduced the concept of the 4D-PET Maximum Intensity Projection (4D-PET MIP) and showed that the 4D-PET MIP accurately measured the motion of FDG-avid primary lung tumors[16]. In this article we explore the utility of a 4D-PET MIP used in conjunction with the end-exhale and end-inhale phases of 4D-PET to construct motion-specific target volumes for malignant FDG-avid lymph nodes, and determine whether such target volumes differ from those generated by standard of care techniques.

Materials and Methods

Imaging

Eleven patients with FDG-avid thoracic tumors were imaged at the Center for Clinical Imaging Research, Mallinckrodt Institute of Radiology (Washington University, Saint Louis, MO), as part of an IRB-approved 4D-PET research protocol. Five of these patients were found to have a total of 11 FDG-avid mediastinal and/or hilar lymph nodes, and are the subject of the present study. Each patient underwent a 12-minute list-mode PET acquisition, a breath-hold CT, and an amplitude-sorted 4D-CT. An abdominal bellows respiratory surrogate (Philips Medical Systems) was acquired simultaneously with the imaging. Approximately 10 mCi of FDG activity was injected into the patient approximately 75 minutes prior to PET imaging. The PET list-mode was gated according to the amplitude of the abdominal bellows into six images. Gating windows were chosen such that each gated image had approximately equal counting statistics. The fact that in normal human breathing more time is spent at end-exhale means that if gating windows are designed to have equal number of events, they will have uneven amplitude ranges, potentially large at end-inhalation, resulting in more intra-gate motion. Conversely, if windows are chosen to subtend equal amplitude ranges, they may have low statistics at the end-inhalation phases and therefore have excess noise. This issue has been examined by Dawood et al for respiratory-gated cardiac PET[17]. They found that the two methods resulted in practically equivalent measured heart displacement, and concluded that equal-events amplitude gating was preferred because of the uniform noise performance per window. Attenuation correction was computed using the best-matching 4D-CT phase according to mean bellows amplitude. An un-gated PET scan was also reconstructed, from the first 3 minutes of list-mode data. The breath-hold CT scan was used for attenuation correction of the un-gated PET.

Target Volume Delineation

Two sets of volumes were contoured for the targeted nodes of each patient. The first, standard-of-care, set of volumes (referred to as the NTV_{3D}) was contoured using conventional un-gated PET, 4D-CT, and breath-hold CT. The NTV_{3D} were then expanded by uniform margins to generate a series of ITV_{3D} volumes. A series of exploratory margins expansions of 5 mm, 8 mm, 10 mm and 13 mm (as well as zero margin addition) were investigated, following recommendations from literature exploring lymph node motion with 4D-CT[8,9]. The second, motion-specific, set of volumes (referred to as ITV_{4DPET}) was contoured using 4D-PET, 4D-CT, and breath-hold CT. The end-exhale, end-inhale, and 4D PET-MIP images were used for 4D contouring. The NTV_{3D} and ITV_{4D} both were drawn to encompass regions of FDG avidity that corresponded to lymph nodes as determined by CT, based on visual interpretation by a radiation oncologist. Contours were drawn to include lymph node motion as measured by 4D-CT when lymph nodes were clearly visible in 4D-CT images.

Analysis

The relative volumes of the ITV_{4D} and NTV_{3D} were used to indicate the magnitude of motion that was explicitly encapsulated in the 4D PET images but not necessarily included in un-gated PET volumes. The volume of ITV_{4D} that was not covered by the ITV_{3D} corresponds to the magnitude of under-dosing, if the true motion of lymph nodes is accurately represented by the 4D-PET motion. Conversely, volume included in ITV_{3D} but not in ITV_{4D} corresponds to presumed healthy tissue that would be unnecessarily irradiated if ITV_{3D} was used.

Results

FDG-avid nodal regions were on average 2.4+−1.3 times greater in the union of 4D-PET images (ITV_{4D}, which explicitly encapsulated node motion) than in the un-gated PET images (NTV_{3D}; refer to Table 1). A 5 mm expansion on the NTV_{3D} only covered the ITV_{4D} in 3 of 11 (27%) nodes, while a 13 mm expansion on the NTV_{3D} was necessary to cover the ITV_{4D} in 10 of 11 (91%) nodes (Table 2). For a 13 mm expansion, the ITV_{3D} were on average 16+-9 times larger than the corresponding ITV_{4D}, but still did not completely cover the ITV_{4D} of one highly-mobile node, missing an absolute volume of 0.26 cm^3 of the ITV_{4D} (12% of ITV_{4D}). On average, the ITV_{3D} generated with 13 mm margins included 45+-34 cm^3 of tissue that was not FDG-avid according to ITV_{4D} (Table 3).

Discussion

Lymph node motion was readily visible in 4D-PET images. The degree of motion observed here was consistent with that described in published reports. Motion-specific internal target volumes were readily drawn using 4D-PET. Use of the 4D-PET MIP is a significant time-saving device, because contouring on the MIP plus end-exhale and inhale 4D-PET phases is expected to take roughly half as long as contouring on all phases of 4D-PET, since 6-8 phases are typically used in 4D-PET imaging[18,19]. We demonstrated that the 4D-PET MIP can be used in conjunction with the end-exhale and end-inhale phases of 4D-PET to construct motion-specific target volumes for malignant FDG-avid lymph nodes, and that such target volume differ at a clinically significant level from those generated by standard of care techniques (non-contrast 4D-CT and breath-hold CT in conjunction with un-gated PET). Our findings are in concordance with similar results on the clinical utility of 4D-PET reported by Aristophanous et al[15]. Our work expands on that presented by those authors in that we calculate for these data the margins needed to expand un-gated PET volumes to cover the observed 4D-PET volumes, and we calculate the corresponding over-coverage, or unnecessary targeting of presumed healthy tissue, that is avoided by using 4D-PET based target volumes. Mohammed et al[20] contoured nodal ITVs in a planning 4D-CT and and found that margins of 8 mm +- 3mm were needed to cover the nodal volumes as imaged on weekly 4D-CT in a scenario where image guidance was performed using bony anatomy or a hybrid image registration to the tumor and involved nodes. That could have resulted in part from the fact that 4D-CT samples node motion over a small time (a single node would be covered by 4D-CT in less than 15 seconds). An additional benefit of 4D-PET could be that it samples tumor motion over the time of the entire PET bed imaging, 12 minutes in our study. That could help capture variations in tumor motion amplitude and baseline; for example, Shah et al observed deviations in mean target position of greater than 2 mm in 40.1% of patients and greater than 5 mm in 7% of patients by comparing pre- and post-treatment CBCT[21]. It is well documented that 4D-PET results in higher standardized uptake values for moving lesions, compared to 3D-PET, through the reduction of motion blurring. Motion blurring could reduce lesion detectability[22] and could either increase or decrease the contoured nodal volume depending on the node uptake and window-level settings used for contouring. It has also been suggested that the motion blurring of un-gated PET could be used to define ITVs for primary lung tumors without 4D-CT[23]. Results of the present study indicate that 4D-PET (which used phase-matched 4D-CT for attenuation correction) is more accurate for ITV generation in the context of FDG-avid mediastinal and hilar lymph nodes.

Because of the degree of motion (up to 1 cm and greater), the variability of motion between different nodes, and the anisotropy of motion (dominantly superior-inferior but with non-negligible components in the anterior-posterior and left-right directions in some nodes), the use of population-based motion margins for lymph nodes results in unnecessary irradiation

of healthy tissue. Where available, 4D-PET should be preferred for generation of motion-specific internal target volumes. Especially for nodes of small volume, the degree of over-coverage of the ITV caused by using population-based margins can be dramatic (for example, see figure 1). A limitation of the present work is that it was not explored to what degree smaller treatment fields would result from the smaller ITVs, due to limitations of minimum field size and of the treatment planning and delivery processes for fractionated lung treatments. Controversy remains regarding the correct method of segmenting PET images[24-26]. In the present paper we have relied on manual segmentation by an experienced radiation oncologist, as is standard practice in our clinics. The PET window-level settings were adjusted by the oncologist on a per-patient and per-image basis in order to include all tissue with uptake above the background level of the mediastinum. The role of automated segmentation algorithms and the addition of appropriate margins to account for PET segmentation uncertainty are the subjects of future work. In analogy with the historical development of 4D-CT in which motion-specific margins for the primary tumor enabled reduction in normal-tissue complication and dose escalation, it can be hoped that the use of 4D-PET will result in similar advances for treatment of node-positive lung cancer.

Acknowledgments

This work is supported in part by NIH R01CA096679 and R01CA116712.

References

1. Dillman RO, Herndon J, Seagren SL, Eaton WL, Green MR. Improved Survival in Stage III Non-Small-Cell Lung Cancer: Seven-Year Follow-up of Cancer and Leukemia Group B (CALGB) 8433 Trial. J Natl Cancer Inst. 1996; 88:1210–1215. [PubMed: 8780630]
2. Sause WT, Byhardt RW, Curran WJ, et al. Follow-up of non-small cell lung cancer. American College of Radiology. ACR Appropriateness Criteria. Radiology. 2000; 215(Suppl):1363–1372. [PubMed: 11037552]
3. Aupérin A, Le Péchoux C, Rolland E, et al. Meta-Analysis of Concomitant Versus Sequential Radiochemotherapy in Locally Advanced Non-Small-Cell Lung Cancer. J. Clin. Oncol. 2010; 28:2181–2190.
4. Rosenzweig KE, Sura S, Jackson A, Yorke E. Involved-Field Radiation Therapy for Inoperable Non- Small-Cell Lung Cancer. J Clin Oncol. 2007; 25:5557–5561. [PubMed: 17984185]
5. Sulman E, Komaki R, Klopp A, Cox J, Chang J. Exclusion of elective nodal irradiation is associated with minimal elective nodal failure in non-small cell lung cancer. Radiation Oncology. 2009; 4:1–7. [PubMed: 19138400]
6. Donnelly ED, Parikh PJ, Lu W, et al. Assessment of Intrafraction Mediastinal and Hilar Lymph Node Movement and Comparison to Lung Tumor Motion Using Four-Dimensional CT. Int J Radiat Oncol Biol Phys. 2007; 69:580–588. [PubMed: 17869671]
7. Pantarotto JR, Piet AHM, Vincent A, van Sörnsen de Koste JR, Senan S. Motion Analysis of 100 Mediastinal Lymph Nodes: Potential Pitfalls in Treatment Planning and Adaptive Strategies. Int J Radiat Oncol Biol Phys. 2009; 74:1092–1099. [PubMed: 19095370]
8. Senan S, De Ruysscher D, Giraud P, et al. Literature-based recommendations for treatment planning and execution in high-dose radiotherapy for lung cancer. Radiother Oncol. 2004; 71:139–146. [PubMed: 15110446]
9. Sher DJ, Wolfgang JA, Niemierko A, Choi NC. Quantification of Mediastinal and Hilar Lymph Node Movement Using Four-Dimensional Computed Tomography Scan: Implications for Radiation Treatment Planning. Int J Radiat Oncol Biol Phys. 2007; 69:1402–1408. [PubMed: 17920783]
10. Yamamoto T, Langner U, Loo BW, Shen J, Keall PJ. Retrospective Analysis of Artifacts in Four-Dimensional CT Images of 50 Abdominal and Thoracic Radiotherapy Patients. Int J Radiat Oncol Biol Phys. 2008; 72:1250–1258. [PubMed: 18823717]

11. Underberg RWM, Lagerwaard FJ, Slotman BJ, Cuijpers JP, Senan S. Use of maximum intensity projections (MIP) for target volume generation in 4DCT scans for lung cancer. Int J Radiat Oncol Biol Phys. 2005; 63:253–260. [PubMed: 16111596]
12. Bradley JD, Nofala AN, Naqa IME, et al. Comparison of helical, maximum intensity projection (MIP), and averaged intensity (AI) 4D CT imaging for stereotactic body radiation therapy (SBRT) planning in lung cancer. Radiother Oncol. 2006; 81:264–268. [PubMed: 17113668]
13. MacManus M, Nestle U, Rosenzweig KE, et al. Use of PET and PET/CT for Radiation Therapy Planning: IAEA expert report 2006–2007. Radiother Oncol. 2009; 91:85–94. [PubMed: 19100641]
14. Park SJ, Ionascu D, Killoran J, et al. Evaluation of the combined effects of target size, respiratory motion and background activity on 3D and 4D PET/CT images. Phys Med Biol. 2008; 53:3661. [PubMed: 18562782]
15. Aristophanous M, Berbeco RI, Killoran JH, et al. Clinical Utility of 4D FDG-PET/CT Scans in Radiation Treatment Planning. Int J Radiat Oncol Biol Phys. 2012; 82:e99–e105. [PubMed: 21377285]
16. Lamb JM, Robinson C, Bradley J, et al. Generating lung tumor internal target volumes from 4D-PET maximum intensity projections. Med Phys. 2011; 38:5732–5737. [PubMed: 21992387]
17. Dawood M, Büther F, Lang N, Schober O, Schäfers KP. Respiratory gating in positron emission tomography: A quantitative comparison of different gating schemes. Med Phys. 2007; 34:3067–3076. [PubMed: 17822014]
18. Bettinardi V, Rapisarda E, Gilardi MC. Number of partitions (gates) needed to obtain motion-free images in a respiratory gated 4D-PET/CT study as a function of the lesion size and motion displacement. Med Phys. 2009; 36:5547–5558. [PubMed: 20095267]
19. Dawood M, Buther F, Stegger L, et al. Optimal number of respiratory gates in positron emission tomography: A cardiac patient study. Med Phys. 2009; 36:1775–1784. [PubMed: 19544796]
20. Mohammed N, Kestin L, Grills I, et al. Comparison of IGRT Registration Strategies for Optimal Coverage of Primary Lung Tumors and Involved Nodes Based on Multiple Four-Dimensional CT Scans Obtained Throughout the Radiotherapy Course. Int J Radiat Oncol Biol Phys. 2012; 82:1541–1548. [PubMed: 21664070]
21. Shah C, Grills IS, Kestin LL, et al. Intrafraction Variation of Mean Tumor Position During Image-Guided Hypofractionated Stereotactic Body Radiotherapy for Lung Cancer. Int J Radiat Oncol Biol Phys. 2012; 82:1636–1641. [PubMed: 21489715]
22. García Vicente AM, Castrejón AS, León Martín AA, García BG, Pilkington Woll JP, Muñoz AP. Value of 4-Dimensional 18F-FDG PET/CT in the Classification of Pulmonary Lesions. J Nucl Med Technol. 2011; 39:91–99. [PubMed: 21565957]
23. Chang G, Chang T, Pan T, Clark JW, Mawlawi OR. Determination of Internal Target Volume From a Single Positron Emission Tomography/Computed Tomography Scan in Lung Cancer. Int J Radiat Oncol Biol Phys. 2012; 83:459–466. [PubMed: 22197228]
24. Biehl KJ, Kong FM, Dehdashti F, et al. 18F-FDG PET Definition of Gross Tumor Volume for Radiotherapy of Non–Small Cell Lung Cancer: Is a Single Standardized Uptake Value Threshold Approach Appropriate? J Nucl Med. 2006; 47:1808–1812. [PubMed: 17079814]
25. Wahl RL, Herman JM, Ford E. The Promise and Pitfalls of Positron Emission Tomography and Single-Photon Emission Computed Tomography Molecular Imaging–Guided Radiation Therapy. Semin Radiat Oncol. 2011; 21:88–100. [PubMed: 21356477]
26. Hatt M, Cheze Le, Rest C, Albarghach N, Pradier O, Visvikis D. PET functional volume delineation: a robustness and repeatability study. European Journal of Nuclear Medicine and Molecular Imaging. 2011; 38:663–672. [PubMed: 21225425]

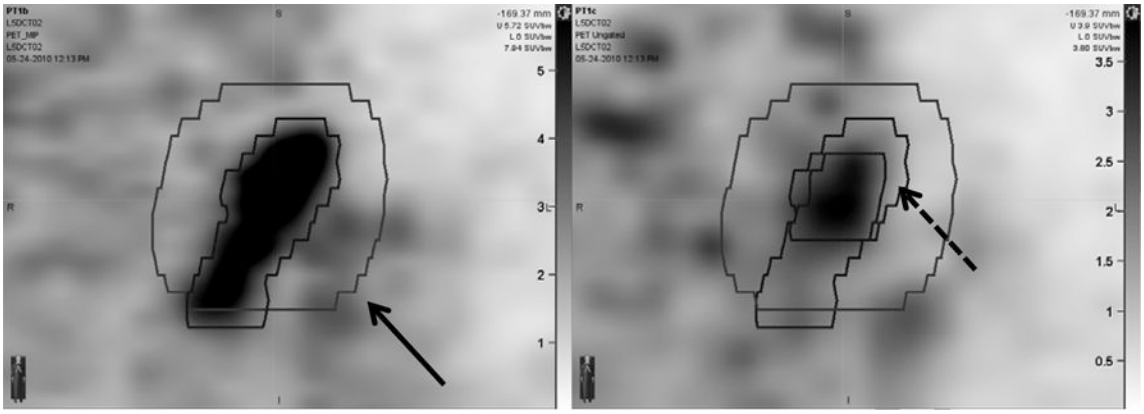

Figure 1.

4D-PET MIP image (left) and un-gated PET image (right) of a para-aortic lymph node (node 1 of patient 2). Internal target volumes based on 4D-PET and on un-gated PET with a 1 cm expansion (solid arrow) are shown superimposed. The un-expanded contour drawn on the un-gated PET image is shown on the right panel (dashed arrow). The intensity scale on the left panel ranges from 0 to 5.73 SUV. The intensity scale on the right panel ranges from 0 to 3.9 SUV. Intensity scales for this display were chosen to match background levels in the PET-MIP and un-gated PET images. Contouring was performed with dynamically adjusted window-level settings.

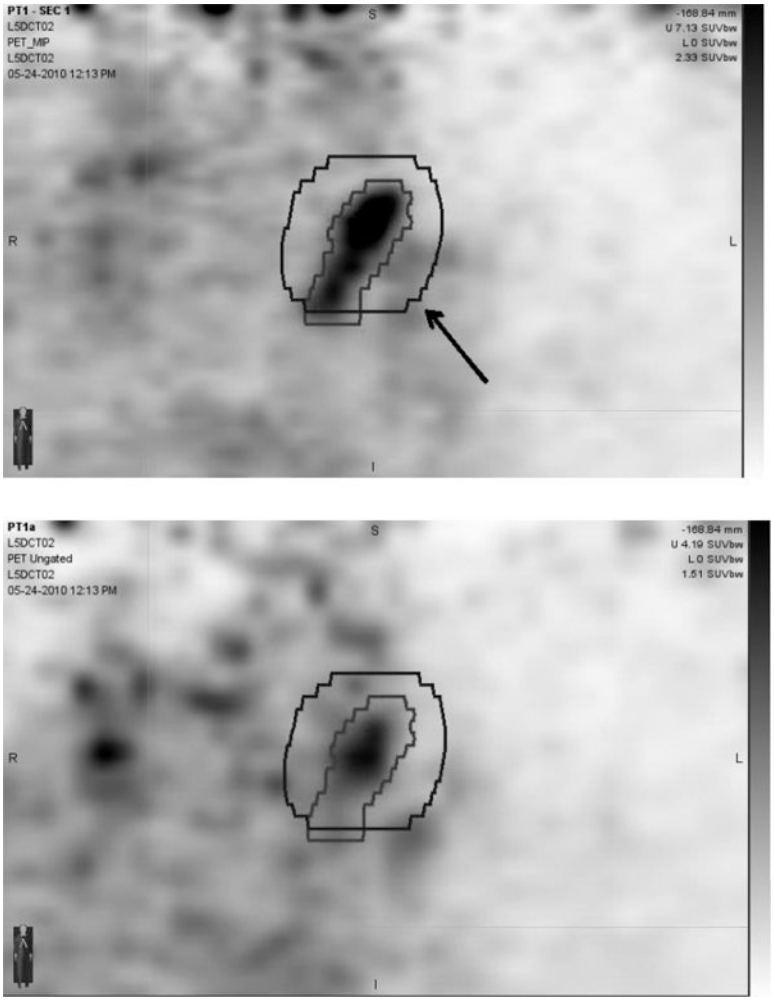

Figure 2. Alternative To Be Used For Figure 1 If Preferred For Formatting

4D-PET MIP image (upper pane) and un-gated PET image (lower pane) of a para-aortic lymph node (node 1 of patient 2). Internal target volumes based on 4D-PET and on un-gated PET with a 1 cm expansion (arrow) are shown superimposed.

Table 1

FDG-avid node motion and nodal volumes measured with un-gated and 4D-PET techniques. Node motion is quantified by the distance between the volume center of mass in the end-exhale and end-inhale phase of 4D-PET.

Patient	Node	Motion (mm)			$V(NTV_{3D})$ (cc)	$V(ITV_{4D})$ (cc)	$V(ITV_{4D})/V(NTV_{3D})$
		AP	LR	SI			
1	1	0.5	4.8	10	0.7	2.5	3.4
	2	0.9	1.1	8.2	7.0	16.2	2.3
2	1	8.6	1.5	17	2.0	5.1	2.5
	2	2.4	1.1	20	0.4	2.2	5.8
3	1	1.3	0.3	3.4	0.4	0.9	2.2
	2	1.8	0.3	0.7	0.5	1.1	2.1
4	1	0.2	1.5	3.9	2.2	2.2	1.0
	2	2.5	0.0	4.6	0.9	1.3	1.5
	3	2.2	0.9	6.7	0.8	1.9	2.4
5	1	0.7	1.3	16	2.54	4.8	1.9
	2	2.1	2.4	9.8	36.78	58.0	1.6

Radiother Oncol. Author manuscript; available in PMC 2014 October 01.

Table 2

Under-coverage (volume of ITV_{4D} missed by the ITV_{3D}) as a function of the margin expansion used to compute the ITV_{3D} from the FDG-avid nodal target volume in un-gated PET (NTV_{3D}).

Patient	Node	Under-overage for Given NTV_{3D}->ITV_{3D} Margin (cm^3)				
		0 mm	5 mm	8 mm	10 mm	13 mm
1	1	1.74	0.33	0.06	0.00	0.00
	2	9.76	2.4	0.24	0.00	0.00
2	1	3.25	1.1	0.66	0.27	0.00
	2	1.85	0.86	0.70	0.52	0.26
3	1	0.55	0.02	0.00	0.00	0.00
	2	0.63	0	0.00	0.00	0.00
4	1	0.45	0	0.00	0.00	0.00
	2	0.44	0	0.00	0.00	0.00
	3	1.17	0.06	0.00	0.00	0.00
5	1	2.29	0.16	0.00	0.00	0.00
	2	21.19	1.5	0.15	0.00	0.00

Radiother Oncol. Author manuscript; available in PMC 2014 October 01.

Table 3

Over-coverage (volume of ITV_{3D} that is not included in ITV_{4D}) as a function of the margin expansion used to compute the ITV_{3D} from the FDG-avid nodal target volume in un-gated PET (NTV_{3D}).

Patient	Node	Over-coverage for Given NTV_{3D}->ITV_{3D} Margin (cm^3)				
		0 mm	5 mm	8 mm	10 mm	13 mm
1	1	0.02	4.1	10	16	28
	2	0.55	10	22	35	59
2	1	0.15	7.0	15	24	39
	2	0.02	3.0	7.9	13	23
3	1	0.07	3.4	8.5	14	24
	2	0.09	3.9	9.4	15	26
4	1	0.48	10	21	31	49
	2	0.03	5.3	12	18	31
	3	0.03	4.6	11	18	31
5	1	0.00	7.2	16	25	42
	2	0.00	30	64	92	140